Enhancement of the Seebeck Coefficient of C doped SnSe: First Principles Study

Ho Van Binh, Nguyen Huynh Tuan Anh, Do Duc Cuong[*]

Use your smartphone to scan this
QR code and download this article

ABSTRACT

The effect of C dopant on the electronic structure and thermoelectric properties of SnSe has been studied using density functional theory (DFT) and by solving the Boltzmann transport equation (BTE). We found that the substitution of C into the Sn site creates a strongly localized defect state with a sharp density for the state peak. This strong modification of band structure reduces the band gap from 0.61 eV to 0.42 eV. It was found that the maximal Seebeck coefficient can be enhanced up to 17.1% and the maximal temperature reduces from 525 K to 280 K. These behaviors can be understood using the Mott equation and Goldsmid – Sharp relation.

Key words: Density functional theory, Boltzmann Transport Equation, Thermoelectric properties, Seebeck coefficient, SnSe

Department of Physics and Computer Science, Faculty of Physics and Engineering Physics, University of Science, VNU-HCM, Ho Chi Minh City, 70000, Vietnam

Correspondence

Do Duc Cuong, Department of Physics and Computer Science, Faculty of Physics and Engineering Physics, University of Science, VNU-HCM, Ho Chi Minh City, 70000, Vietnam

Email: ddcuong@hcmus.edu.vn

Check for updates

VNUHCM PRESS

INTRODUCTION

The demand for new sources of energy has been increased rapidly recently because of the increasing price and emissions of traditional energy sources (fossil fuels, gases et al.). On the other hand, the current technologies are not effective because up to 60% of the energy is released in the form of waste heat[1]. In the search for new sources of energy, thermoelectric materials have received much attention owing to their capability to convert thermal energy into electrical energy. Despite a long history of development, current state of art thermoelectrics are still insufficient for wide-scale application due to their low conversion efficiency and high-cost materials. Finding new thermoelectric materials with a high performance and use of non-toxic and low-cost materials is a challenge faced by thermoelectric research activities. The efficiency of thermoelectric materials is strongly related to dimensionless figure of merit, which is defined by $ZT = \frac{\sigma S^2}{\kappa} T = \frac{PF}{\kappa} T$ where σ, S, κ, and T are electrical conductivity, the Seebeck coefficient, thermal conductivity, and absolute temperature, respectively. PF=$\sigma \cdot S^2$ defines the power factor[1]. Practical applications often require large ZT materials, meaning that they should have both a large power factor (S and σ) and small thermal conductivity (κ). However, obtaining high ZT materials is the challenge because of the non-trivial interplay between σ, κ, and S[2]. For example, in most cases, when σ increases, S decreases and κ increases, and vice versa. The best commercial thermoelectric materials currently used in devices

are Bi_2Te_3 and its alloys where the ZT is about 1.0, corresponding to an efficiency of less than 10%. This value has been a practical upper limit for more than 30 years. Therefore, suitable approaches should be undertaken to obtain a higher ZT.

Recently, Zhao et. at. found that the ZT of the single crystal SnSe was up to 2.6 at 923 K due to its intriguing electrical properties and extremely low thermal conductivity, making this material the most promising thermoelectric material for device realization[3]. This is fascinating because SnSe is composed of two abundant and environmentally friendly elements: Sn and Se. More importantly, the extremely low thermal conductivity of single crystal SnSe is beneficial because now, most complex procedures to reduce the thermal conductivity can be avoided and allow for a focus mainly on increasing the power factor[4]. However, the thermoelectric properties of SnSe near room temperature are still very low ($\sim$0.1). Doping SnSe could be a good solution to enhance the thermoelectric properties of SnSe near room temperature. Several dopants have been studied, aiming to modify the electronic structure and then improve the thermoelectric performance of this material[5–8]. For example, Na-doped SnSe can enhance the ZT from 0.1 to 0.7 near room temperature[9]. By doping n-type Bi elements into SnSe, Tuan et. al. obtained an n-type SnSe with a ZT up to 2.2 at 733 K[10]. Another doped system, Br-doped SnSe, was found to improve the ZT up to 2.8 at 773 K[11]. In this study, we have systematically investigated the effect of the isoelectronic C dopant on the electronic structure and thermoelectric

of SnSe. We expected that the isoelectronic doping of SnSe may cause a big modification of the electronic structure near the Fermi level and enhance the electrical and thermoelectric properties of this material.

MATERIALS AND METHODS

The first-principles density functional calculations were performed using the Vienna Ab Initio Simulation Package (VASP)[12]. For the exchange-correlation potential, a generalized gradient approximation (GGA) was employed with Perdew, Burke, and Ernzerhof (PBE) parametrization[13,14] and projected augmented wave (PAW) basis sets[15]. The cutoffs for kinetic energy were chosen at 450 eV. To consider the isoelectronic doping in SnSe, we replaced one Sn by C in the $1\times2\times2$ supercell (containing total 32 atoms) corresponding to stoichiometry $Sn_{1-\delta}SeC_\delta$ with δ = 0.0625 (or 6.25%). The structure was then fully relaxed with the force criteria being 0.001 eV/atom. The thermoelectric properties were calculated using BoltzTrap[16] where the band eigenvalues were interpolated to extract the velocities based on the converged electronic structure. More specifically, the interpolation was done on a k-grid of $8\times8\times8$ giving 128 k-points in the irreducible Brillouin zone wedge. The Seebeck coefficient (or thermopower), S, was expressed as:

$$S_{\alpha\beta}(\mu,T) = \frac{1}{eT} \frac{L^1_{\alpha\beta}(\mu,T)}{L^0_{\alpha\beta}(\mu,T)}$$

where α and β denote x, y,z; μ is the chemical potential, e is the electron charge; T is temperature, and the L^0 and L^1 tensors represent the transport distribution function:

$$L^n_{\alpha\beta}(\mu,T) = \sum_k \tau(k)\, v_\alpha(k)\, v_\beta k \left(\frac{-\partial f(\varepsilon)}{\partial \varepsilon}\right)(\varepsilon(k)-\mu)^n$$

Where ε(k) is the band eigenvalues, $v_\alpha(\kappa) = \frac{1}{h}\frac{\partial \varepsilon(\kappa)}{\kappa_\alpha}$ $(\alpha = x,y,z)$ is the group velocity, τ(k) is the relaxation time, and f(ε) is the Fermi-Dirac distribution function. Since τ is not well known in general, the Seebeck coefficient is evaluated within a constant relaxation time approximation, which reads:

$$S_{\alpha\beta}(\mu,T) = \frac{\sum_k v_\alpha(k) v_\beta(k)\left(\frac{-\partial f(\varepsilon)}{\partial \varepsilon}\right)(\varepsilon(k)-\mu)}{\sum_k v_\alpha(k) v_\beta(k)\left(\frac{-\partial f(\varepsilon)}{\partial \varepsilon}\right)}$$

For the doping system, the Fermi level is shifted on top of the valence band and the doping concentration is taken into account by changing the chemical potential μ.

RESULTS

At room temperature, SnSe crystallizes in a GeS-type orthorhombic structure with space group Pnma(#62) and undergoes a structural phase transition to a TlI-type rhombohedral structure with space group Cmcm (#63) at T = 807 K. The structure of SnSe is composed of double layers separated by weak Van der Waals bonding along the a-direction as shown in Figure 1(a). Each Sn atom forms three covalent bonds with Se, which is the same for the Se atom. In each layer, Sn and Se form a buckling two-dimensional chain where three bonds, one vertical and two equivalent horizontal bonds, are denoted as (1) and (2). The experimental lattice parameters are a = 11.501 Å, b = 4.445 Å, c = 4.153 Å with bond lengths of 2.793 Å and 2.744 Å for the vertical and horizontal bonds, respectively, indicating an anisotropic bond length[17]. Our optimized lattice constants were a = 11.778 Å, b = 4.569 Å and c =4.216 Å, which are overestimated with respect of the experimental one by about 2.7%, 1.5% and 2.4%. The calculated Sn-Se bond lengths for the vertical and horizontal bonds are 2.83 Å (1) and 2.79 Å (2), which is about 1.2% and 1.6% bigger than in the experiment. This overestimation of the lattice parameters and bond lengths is well-known in GGA approximation[18].

Figure 1(b) and (c) compare the band structures of pristine SnSe and C doped SnSe where the contribution of each orbital in the band is represented by different colors and sizes. We found that pristine SnSe shows semiconductor behavior with an indirect band gap of 0.61 eV. The valence band maximum (VBM) is located at **k**= (0.00, 0.33, 0.00) along Y-Γ direction in a direct reciprocal lattice, while the conduction band minimum (CBM) is at **k**= (0.00, 0.00, 0.33) along Z-Γ direction. The direct band gap, or the optical gap, is 0.87 eV which occurs at **k**= (0.00, 0.00, 0.33) along the Z-Γ direction. The magnitudes of both indirect and direct gaps are underestimated compared to the experiment (where the indirect and direct band gaps are 0.989 eV and 1.238 eV, respectively[19]), consistent with the previous calculations[20,21]. VBM is contributed to mainly by the Se $4p_y$ states, while the main contributions of CBM are found in the Sn $5p_x$, $5p_z$ states[22]. The Valence band maximum (VBM) and Conduction band minimum (CBM) of the C doped SnSe system does not change much due to the similarity of the electronic character between C and Sn. However, we found that C creates quite a flat localized defect state in the band gap region while the valence band does not change much. The Fermi level is shifted
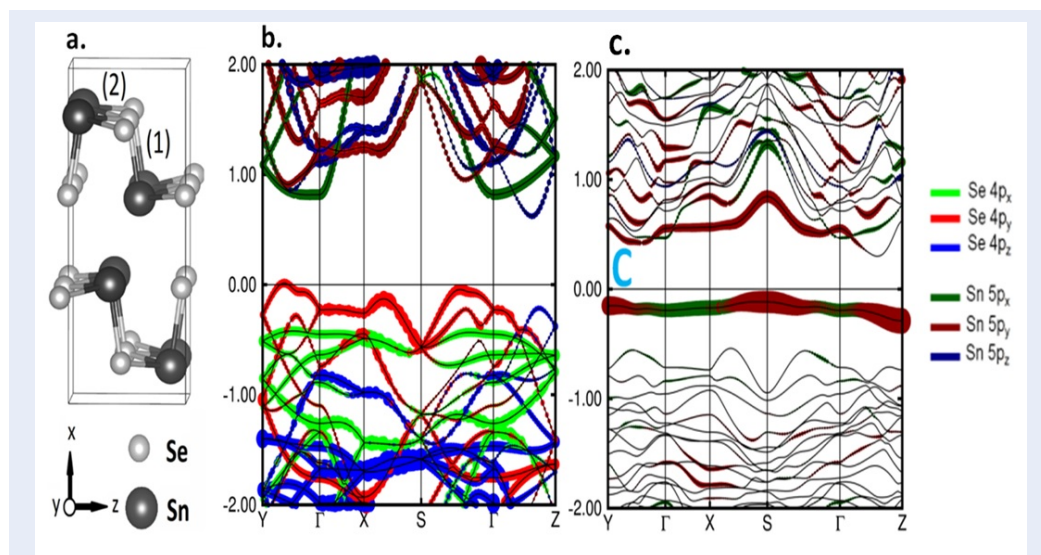
Figure 1: (a) One unit cell of SnSe in an orthorhombic structure; (b) the band structure of pristine SnSe in a $1\times2\times2$ supercell; (c) the band structure of C doped SnSe. The Fermi level is scaled at a zero energy level and the color circle represents the contribution of orbitals; a bigger circle means more contribution by the orbital.
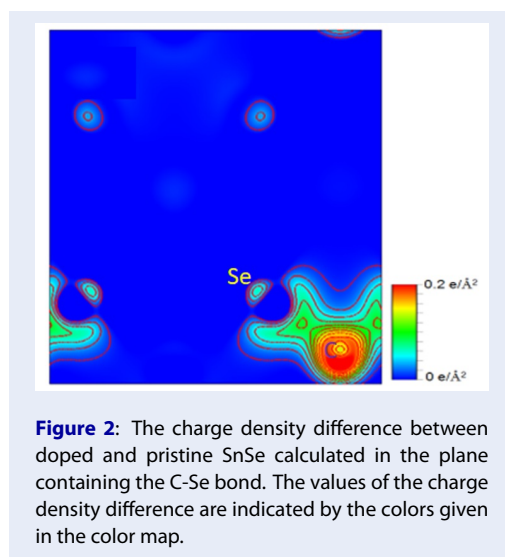

Figure 2: The charge density difference between doped and pristine SnSe calculated in the plane containing the C-Se bond. The values of the charge density difference are indicated by the colors given in the color map.

above the localized state, resulting in the strong reduction of the band gap from 0.61 eV (in pristine SnSe) to 0.42 eV in the doped system.

To understand the details of the electronic behavior of C dopant, in Figure 2, we show the charge density difference between the doped system and pristine one. We found that many charges concentrate near the C atom with some extending toward the surrounding Se atoms. We note that the electronegativity of C is 2.55, which is much larger than that of its substituted atom Sn (1.8) and even bigger than that of anion Se

(2.4)[23]. Therefore, the C atom substituting into the Sn site tends to gain more electrons from the surrounding atoms than Sn. Due to the smaller difference in electronegativity between C and Se, the charge of C is more extended toward the neighboring Se, indicating that the bonding character of C-Se prefers a covalent bond rather than ionic bond like in the pristine one. In Figure 2, we compare the density of state (DOS) between two systems. It was found that the existence of a localized state in the band gap region in the C doped SnSe system results in a very sharp DOS peak in the band gap as shown in Figure 2(b). The sharp DOS peak plays quite an important role in enhancing the thermoelectric properties of the materials which we will discuss in the next part.

Figure 4 presents the dependence of the Seebeck coefficient at different temperatures calculated at a fixed experimental hole carrier concentration of $6\times10^{17}\text{cm}^{-3}$ [4,20]. The Seebeck coefficient of both systems show a similar trend: it increases from a low temperature and reaches the maximal value (S_{max}) at a certain temperature (T_{max}), rapidly reducing after T_{max} due to the infamous bipolar transport mechanism[24]. Our calculations for the Seebeck coefficient of pristine SnSe in the current study are comparable with previous studies[4,19,22]. Note that the S_{max} of pristine SnSe is about 601.5 S/cm at T_{max} = 525 K which is close to the previous experimental value (about 600 S/cm at T_{max} = 625 K)[3,4]. The difference in the T_{max} of the pristine SnSe between our calculation
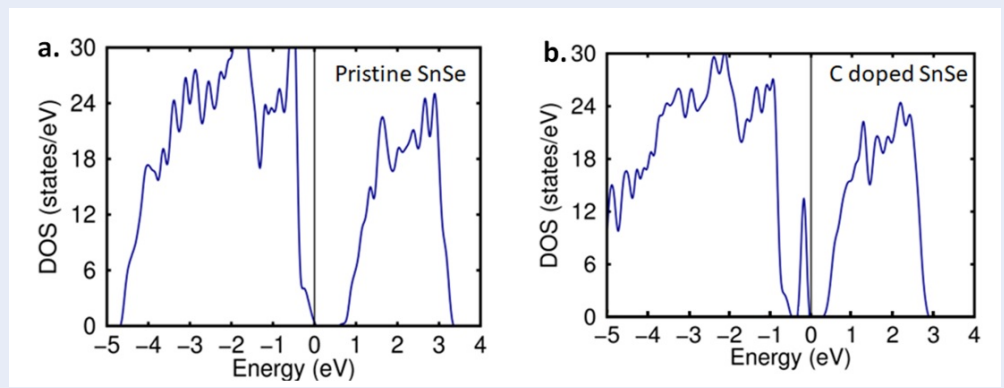
Figure 3: Density of the states of (a) Pristine SnSe and (b) C doped SnSe. The existence of a localized state in the band gap creates a sharp DOS peak in the C doped SnSe system.
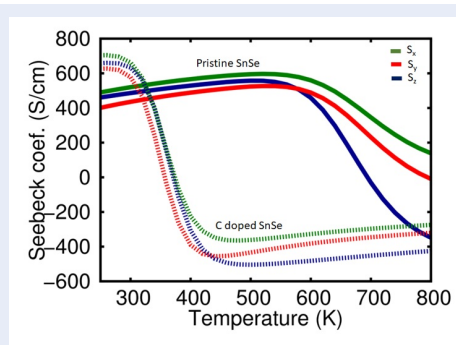
Figure 4: Seebeck coefficient of both pristine SnSe and C doped SnSe with the function temperature of doped SnSe along the x, y, z direction. The dashed lines indicate the Seebeck coefficient of C doped SnSe.

(525 K) and the experiment (625 K) is attributed to the underestimation of the band gap. We found that the S_{max} of C doped SnSe is up to 704.6 S/cm at T_{max} = 280 K, which is about 17.1% enhanced compared to the pristine one.

DISCUSSION

In a previous study, Heremans et al. showed that the ZT of PbTe is improved by doping Tl. This improvement in mostly comes from an increase in the Seebeck coefficient (S), caused by additional Tl-induced DOS peaks[25]. On the other hand, Mahan and Sofo predicted that a sharp increase in the DOS would improve the thermoelectric efficiency by enhancing the Seebeck coefficient[26,27]. The existence of O dopant in ZnSe modified the electronic properties near the Fermi level, pushing up the peak density of the state, and leading to the enhancement of the Seebeck coef-

ficient in O-doped ZnSe[28]. These behaviors can be understood using the Mott formula given by[28]:

$$S = \frac{\pi^2 k_B^2 T}{3q} \left(\frac{1}{\varphi(\varepsilon)} \frac{d\varphi(\varepsilon)}{d\varepsilon} \right)_{\varepsilon=\varepsilon_F}$$

where q is the carrier charge, k_B is the Boltzmann constant, and T is the absolute temperature. $\varphi(\varepsilon)$=D(ε)f$(\varepsilon)\gamma(\varepsilon)$ with D(ε), f$(\varepsilon),\gamma(\varepsilon)$ are the densities of the states, the Fermi distribution, and the energy-dependent mobility, respectively. Note that the derivatives are taken from the Fermi level of energy. The existence of peak DOS can enhance the Seebeck coefficient when a certain carrier concentration is introduced to the system. Therefore, when the concentration of $6\times10^{17} cm^{-3}$ is doped in the C-doped SnSe, it shifts the Fermi level down to the edge of the density of the state peak which can result in a sharp enhancement of the Seebeck coefficient. On the other hand, a reduction of the maximal temperature (T_{max}) can be easily understood using the Goldsmid – Sharp relation, where maximal temperature (T_{max}), band gap (E_g), and the maximal Seebeck coefficient (S_{max}) are related through $E_g = 2e|S_{max}|T_{max}$[22,25,26]. From this relation, the difference in T_{max} between our calculation (525 K) and the experiment (625 K) can be attributed to the underestimation of the band gap. The reduction of T_{max} in C doped SnSe from 525 K to 280 K can be expected due to the large reduction of the band gap from 0.61 eV to 0.42 eV. In fact, the maximal temperature changes depending on the location of localized state in the band gap. It is a well-known problem that the GGA utilized in the current study results in a substantial underestimation of the calculated band gap of SnSe. Therefore, the current maximal temperature can deviate from the experimental one.

CONCLUSION

In the current study, the influences of C dopant on the electronic and thermoelectric properties of an SnSe semiconductor are studied using the first principles calculation and by solving the Boltzmann transport equation. We show that the maximal Seebeck coefficient of C doped SnSe can be enhanced up to 17.1% and that its maximal temperature is reduced from 525 K down to 280 K. These thermoelectric behaviors can originate from the existence of a strong localized state with a sharp DOS peak. This can be understood using the Mott equation and Goldsmid-Sharp relation. Based on the results, the thermoelectric properties of C-doped SnSe are expected to be enhanced toward a lower temperature.

ABBREVIATIONS

DFT: Density functional theory

BTE: Boltzmann transport equation

GGA: Generalized gradient approximation

PAW: Projected augmented wave

ZT: Figure of Merit

PF: Power Factor

σ: electrical conductivity

S: Seebeck coefficient

κ: thermal conductivity

COMPETING INTEREST

The authors declare no competing financial interest.

AUTHORS' CONTRIBUTION

D. D. C conceived of the presented idea. H. V. B and N. H. T. A performed the computations and analyzed data. D. D. C wrote the manuscript with support from H. V. B and N. H. T. A. All authors discussed the results and contributed to the final manuscript.

ACKNOWLEDGEMENT

REFERENCES

1. He J, Kanatzidis MG, Dravid VP. High performance bulk thermoelectrics via a panoscopic approach. Mater Today. 2013;16(5):166-76;Available from: https://doi.org/10.1016/j.mattod.2013.05.004.

2. Snyder GJ, Toberer ES. Complex thermoelectric materials. Nat Mater. 2008;7(2):105-14;PMID: 18219332. Available from: https://doi.org/10.1038/nmat2090.

3. Zhao LD, Lo SH, Zhang Y, Sun H, Tan G, Uher C et al. Ultralow thermal conductivity and high thermoelectric figure of merit in SnSe crystals. Nature. 2014;508(7496):373-7;PMID: 24740068. Available from: https://doi.org/10.1038/nature13184.

4. Zhao L, Chang C, Tan G, Kanatzidis MG. SnSe: a remarkable new thermoelectric material. Energy Environ Sci. 2016;9(10):3044-60;Available from: https://doi.org/10.1039/C6EE01755J.

5. Chen S, Cai K, Zhao W. The effect of Te doping on the electronic structure and thermoelectric properties of SnSe. Phys B. 2012;407(21):4154-9;Available from: https://doi.org/10.1016/j.physb.2012.06.041.

6. Li P, Ai X, Zhang Q, Gu S, Wang L, Jiang W. Enhanced thermoelectric performance of hydrothermally synthesized polycrystalline Te-doped SnSe. Chin Chem Lett. 2021;32(2):811-5;Available from: https://doi.org/10.1016/j.cclet.2020.04.046.

7. Patel S, Chaki SH, Vinodkumar PC. Effect of sulphur doping in SnSe single crystals on thermoelectric power. Mater Res Express. 2019;6(8):085910;Available from: https://doi.org/10.1088/2053-1591/ab1d9d.

8. Gharsallah M, Serrano-Sánchez F, Nemes NM, Mompeán FJ, Martínez JL, Fernández-Díaz MT et al. Giant Seebeck effect in Ge-doped SnSe. Sci Rep. 2016;6:26774;PMID: 27251233. Available from: https://doi.org/10.1038/srep26774.

9. Zhao LD, Tan G, Hao S, He J, Pei Y, Chi H et al. Ultrahigh power factor and thermoelectric performance in hole-doped single-crystal SnSe. Science. 2016;351(6269):141-4;PMID: 26612831. Available from: https://doi.org/10.1126/science.aad3749.

10. Duong AT, Nguyen VQ, Duvjir G, Duong VT, Kwon S, Song JY et al. Achieving =2.2 with Bi-doped n-type SnSe single crystals. Nat Commun. 2016;7:13713;PMID: 27941762. Available from: https://doi.org/10.1038/ncomms13713.

11. Chang C, Wu M, He D, Pei Y, Wu CF, Wu X et al. 3D charges and 2D phonon transports leading to high out-of-plane in n-type SnSe crystals. Science. 2018;360(6390):778-83;PMID: 29773748. Available from: https://doi.org/10.1126/science.aaq1479.

12. Kresse G, Hafner J. Ab initio molecular dynamics for liquid metals. Phys Rev B Condens Matter. 1993;47(1):558-61;PMID: 10004490. Available from: https://doi.org/10.1103/PhysRevB.47.558.

13. Perdew JP, Chevary JA, Vosko SH, Jackson KA, Pederson MR, Singh DJ et al. Atoms, molecules, solids, and surfaces: applications of the generalized gradient approximation for exchange and correlation. Phys Rev B Condens Matter. 1992;46(11):6671-87;PMID: 10002368. Available from: https://doi.org/10.1103/PhysRevB.46.6671.

14. Perdew JP, Burke K, Ernzerhof M. Generalized gradient approximation made simple. Phys Rev Lett. 1996;77(18):3865-8;PMID: 10062328. Available from: https://doi.org/10.1103/PhysRevLett.77.3865.

15. Blöchl PEBl. Projector augmented-wave method. Phys Rev B. 1994;50(24):17953-79;PMID: 9976227. Available from: https://doi.org/10.1103/PhysRevB.50.17953:.

16. Madsen GKH, Singh DJ. BoltzTraP. A code for calculating band-structure dependent quantities. Comput Phys Commun. 2006;175(1):67-71;Available from: https://doi.org/10.1016/j.cpc.2006.03.007.

17. Wiedemeier H, Schnering HV. Refinement of the structures of GeSe, GeS, SnS and SnSe. Z Kristallogr. 1978;148:295-304;Available from: https://doi.org/10.1524/zkri-1978-3-410.

18. Borlido P, Schmidt J, Huran AW, Tran F, Marques MAL, Botti S. Exchange-correlation functionals for band gaps of solids: benchmark, reparametrization and machine learning. npj Comp Mater. 2020;6(1):96;Available from: https://doi.org/10.1038/s41524-020-00360-0.

19. Pafak H, et al. Dispersion analysis of SnS and SnSe. Turk J Phys. 2002;26, 341:26.341;.

20. Cuong DD, Rhim SH, Lee J-H, Hong SC. Strain effect on electronic structure and thermoelectric properties of orthorhombic SnSe: A first principles study. AIP Adv. 2015;5(11):117147;Available from: https://doi.org/10.1063/1.4936636.

21. Das A, Kumar A, Banerji P. First principles study of electronic structure and thermoelectric transport in tin selenide and phase separated tin selenide-copper selenide alloy. J Phys Condens Matter. 2020;32(26):265501;PMID: 32106100. Available from: https://doi.org/10.1088/1361-648X/ab7ad8.

22. Shi G, Kioupakis E. Quasiparticle band structures and thermoelectric transport properties of p-type SnSe. Appl Phys. 2015;117(6):065103;Available from: https://doi.org/10.1063/1.4907805.

23. Pauling L. The nature of the chemical bond. 3rd ed. Cornell University; 1960;.

24. Heremans JP, Jovovic V, Toberer ES, Saramat A, Kurosaki K, Charoenphakdee A et al. Enhancement of thermoelectric efficiency in PbTe by distortion of the electronic density of states. Science. 2008;321(5888):554-7;PMID: 18653890. Available from: https://doi.org/10.1126/science.1159725.

25. Kutorasinski K, Wiendlocha B, Kaprzyk S, Tobola J. Electronic structure and thermoelectric properties of n- and p-type SnSe from first-principles calculations. Phys Rev B. 2015;91(20):205201;Available from: https://doi.org/10.1103/PhysRevB.91.205201.

26. Gibbs ZM, Kim H-S, Wang H, Snyder GJ. Band gap estimation from temperature dependent Seebeck measurement-deviations from the 2ème. Appl Phys Lett. 2015;106(2):022112;Available from: https://doi.org/10.1063/1.4905922.

27. Mahan GD, Sofo JO. the best thermoelectric. Proc Natl Acad Sci U S A. 1996;93(15):7436-9;PMID: 11607692. Available from: https://doi.org/10.1073/pnas.93.15.7436.

28. Lee JH, Wu J, Grossman JC. Enhancing the thermoelectric power factor with highly mismatched isoelectronic doping. Phys Rev Lett. 2010;104(1):016602;PMID: 20366377. Available from: https://doi.org/10.1103/PhysRevLett.104.016602.